Planetary and Space Science 59 (2011) 880–885

Contents lists available at ScienceDirect

Planetary and Space Science

journal homepage: www.elsevier.com/locate/pss

Rapid Communication

High-altitude charged aerosols in the atmosphere of Titan

Marykutty Michael [a,*], Sachchida N. Tripathi [b,1], Pratima Arya [a], Andrew Coates [c], Anne Wellbrock [c], David T. Young [d]

[a] Department of Civil Engineering, Indian Institute of Technology Kanpur, India
[b] NASA Goddard Space Flight Center, Greenbelt, USA
[c] Mullard Space Science Laboratory, University College London, London, UK
[d] Space Science and Engineering Division, Southwest Research Institute, San Antonio, USA

ARTICLE INFO

Article history:
Received 19 January 2011
Received in revised form
15 March 2011
Accepted 18 March 2011
Available online 2 April 2011

Keywords:
Titan
Aerosol
Ionosphere
Heavy ion
Charging

ABSTRACT

Observations by several instruments onboard the Cassini spacecraft revealed the existence of heavy hydrocarbon and nitrile species with masses of several thousand atomic mass units in the ionosphere of Titan. These very large molecules are in fact aerosols. The goal of this paper is to compute the concentrations of the charged aerosols in the upper atmosphere (950–1200 km) of Titan. The charging of these aerosols has been studied using the charge balance equations, where positive ions, negative ions, electrons, neutral and charged aerosols are included. Number concentrations of charged aerosols are compared with those observed by the Cassini instruments. The present work estimates the aerosol mass density as 1–10 kg/m^3, which is within the predicted range. The results show that the aerosols must be smaller than 10 nm in order to have reasonable agreement with observations by the Cassini Plasma Spectrometer.

1. Introduction

The thick haze layers in the atmosphere of Titan were detected by infrared and ultraviolet terrestrial observations made about three decades ago (Danielson et al., 1973; Veverka, 1973; Zellner, 1973; Trafton, 1975). Later observations by Voyager 1 and 2 revealed the existence of two principal haze layers (Smith et al., 1981, 1982). The likely cause of the haze-forming aerosols was recognized as photochemistry occurring in the upper atmosphere of Titan (Danielson et al., 1973). Photochemical models by Wilson and Atreya (2004) suggested that the formation of heavy hydrocarbons such as benzene occurs primarily in the well-mixed region of Titan's atmosphere below the homopause, near 750 km. Ion-neutral reactions at higher altitudes were believed to be weaker sources of complex hydrocarbons. Therefore scientists were not expecting detectable amounts of complex hydrocarbons at altitudes above 950 km, the region sampled by the Cassini orbiter during its pass through the Titan's upper atmosphere. Nonetheless, the Ion and Neutral Mass Spectrometer (INMS), Cassini Plasma Spectrometer (CAPS) sensors and Radio and Plasma Wave Science (RPWS) instruments onboard Cassini spacecraft detected a significant population of heavy hydrocarbon and nitrile species, which are the precursors of tholins at altitudes greater than 950 km. INMS observed ion and neutral molecular masses up to 100 amu/e (Waite et al., 2005, 2007) and Ion Beam Spectrometer (IBS) and Electron Spectrometer (ELS), both of which are CAPS sensors, observed negative ions of mass/charge (m/q) up to 13800 amu/e and positive ions up to 350 amu/e (Waite et al., 2007; Coates, 2009; Coates et al., 2007, 2010; Crary et al., 2009). RPWS also detected heavy positive ions of m/q greater than 100 amu/e (Wahlund et al., 2005, 2009). The concentrations of these ions were found to be ~10% as that of electrons in the ionosphere (Coates et al., 2007). The heavy ions are suggested to be aromatic hydrocarbons (Waite et al., 2007; Coates et al., 2007), acetylene and nitrile polymers (Crary et al., 2009) or fullerenes (Sittler et al., 2009).

The heavy molecular ions are believed to be aerosols (Waite et al., 2009; Coates et al., 2009; Wahlund et al., 2009). The heavy ions of mass greater than 100 amu/e observed at altitudes less than 1200 km during T17, T18, T26 and T32 flybys (Crary et al., 2009; Wahlund et al., 2009), have been suggested as precursors of larger aerosols seen at lower altitudes (Tomasko and West, 2009). Lavvas et al. (2008), using a radiative-photochemical-microphysical model revealed a first peak in haze production rate between 100 and 200 km and a second peak between 500 and 900 km in the atmosphere. Lavvas et al. (2009) after analyzing the observations of several Cassini instruments suggest that the aerosol size in the detached haze layer is in the range of 40 nm. The source of the detached haze layer (between 500 and 900 km) was not

* Corresponding author.: Tel.: +91 512 259 8501.
E-mail address: mary@iitk.ac.in (M. Michael).
[1] Permanent address: Department of Civil Engineering, Indian Institute of Technology Kanpur, India.

0032-0633/$ - see front matter © 2011 Elsevier Ltd. All rights reserved.
doi:10.1016/j.pss.2011.03.010

clearly known until Cassini instruments detected the heavy ion population in the ionosphere of Titan. The present work puts constraints on the charges carried by the observed heavy ions (hereafter referred to as aerosols).

Heavy ion concentration was originally reported as 50 cm^{-3} at ~1000 km by Waite et al. (2007) based on UVIS observations and ~100 cm^{-3} by Coates et al. (2007). The heavy ion concentration in the altitude interval of 950–1150 varies between 100–2000 cm^{-3} during Titan flybys at different magnetospheric conditions and different locations in the atmosphere (Wahlund et al., 2009). Liang et al. (2007) using UVIS observations suggested that the heavy ion concentration for altitudes 800–1000 km is about 100 cm^{-3}. These very large molecules are considered as aerosols in the present work and the calculations of the charging of these aerosols have been done at altitudes of 950 and 1120 km and are then compared to those observed by CAPS ELS during T16 (Coates et al., 2007) and T29. The present model attempts to calculate the charge state of these aerosols, which are present at 950–1200 km in the atmosphere. The model also estimates the size and mass density of the aerosol particles and compares them with estimates available in the literature. The numerical scheme used in the model, the processes considered and comparison of m/q with observed data are presented in the following sections.

2. Input data and numerical scheme

Basic inputs for the model are pressure, temperature, neutral concentration, aerosol concentration and aerosol effective radii. The values of pressure, temperature and neutral concentration measured during the entry of the Cassini–Huygens probe into the atmosphere of Titan are used in the present study. Aerosols are considered to be heavy ions with masses more than 100 amu/e observed by INMS and CAPS. The concentrations of these aerosols are taken from Waite et al. (2007, 2009), Coates et al. (2007) and Wahlund et al., (2009). At 950 km, three aerosol concentrations of 50 cm^{-3}, 100 cm^{-3} and 2000 cm^{-3} are considered while 30 cm^{-3} is used at 1120 km. Though the radius of the aerosols was originally deduced as $\leq$260 nm (Waite et al., 2007), it was later inferred that these aerosols can be as small as 38 nm (Waite et al., 2009; Sittler et al., 2009). Therefore at each altitude, distribution of aerosols (polydisperse distribution (Seinfeld and Pandis, 1998)) is considered where the radii vary from 0.5 to 64 nm. Various cases of aerosol distributions have been studied with mean radii varying from 2 to 16 nm at all altitudes. The standard deviation was kept constant at 1.7 for all the distributions. The distribution of aerosols used at 950 km is shown in Fig. 1.

The concentrations of ions (n^+, n^-), electrons (n^e) and aerosols (N) are found from the charge balance equations. These constitute a set of $(2s+1)\times k+3$ simultaneous differential equations, where s is the maximum number of elementary charges allowed on an aerosol and k is the radius index of polydisperse aerosols. The ion and electron charge balance equations can thus be written as

$$\frac{dn^+}{dt} = q-\alpha n^+ n^- - \alpha_e n^+ n^e - n^+ \sum_i \sum_k \beta_{1k}^{(i)} N_k^i \quad (1)$$

$$\frac{dn^-}{dt} = \beta_j n_j n^e - \alpha n^+ n^- - n^- \sum_i \sum_k \beta_{2k}^{(i)} N_k^i \quad (2)$$

$$\frac{dn^e}{dt} = q-\alpha_e n^+ n^e - \beta_j n_j n^e - n^e \sum_i \sum_k \beta_{ek}^{(i)} N_k^i \quad (3)$$

$$\frac{dN^i}{dt} = \beta_{1k}^{(i-1)} n^+ N_k^{(i-1)} + \beta_{2k}^{(i+1)} n^- N_k^{(i+1)} + \beta_{ek}^{(i+1)} n^e N_k^{(i+1)} - \beta_{1k}^{(i)} n^+ N_k^i - \beta_{2k}^{(i)} n^- N_k^i - \beta_{ek}^i n^e N_k^i \quad (4)$$

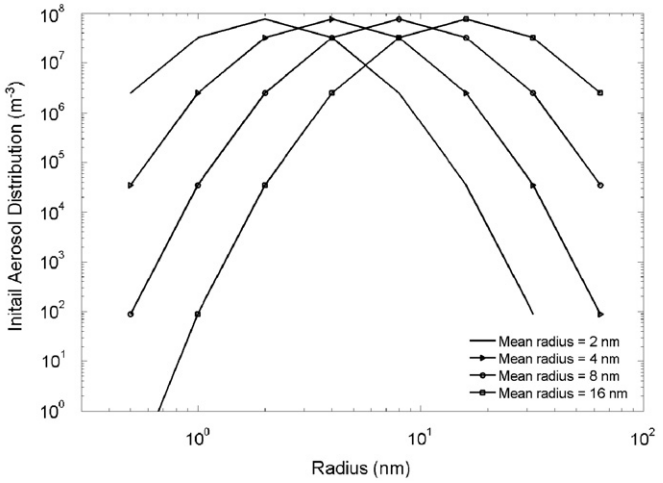

Fig. 1. Distribution of particles used in the model at 950 km in the atmosphere.

here q is the production rate of electrons and positive ions, α is the ion–ion recombination coefficient and α_e is the ion–electron recombination coefficient, β_{mk}^i is the charge transfer coefficient for ions of polarity m (1 for positive and 2 for negative ions) to aerosols with charge i and radius index k, β_{ek}^i is the electron attachment coefficient to aerosols with charge i and radius index k. Negative ions are produced by the electron attachment to the neutrals and β_j is the electron attachment coefficient to neutral species n_j and N_k^i is the concentration of aerosols of charge i and radius index k. β_j used in the present study is 1×10^{-21} m^3 s^{-1}, estimated from the work of Christophorou (1980) and n_j is obtained from Vuitton et al. (2009). The ion–ion recombination coefficient is calculated using the method of Hu and Holzworth (1996).

The production rate of electrons estimated using the CAPS ELS electron densities by Galand et al. (2010) for T18 is used in the present study, which is 2×10^{-1} cm^{-3} s^{-1}. The ion–electron recombination coefficients (6×10^{-6} cm^3 s^{-1} and 1×10^{-6} cm^3 s^{-1} at 950 and 1120 km, respectively) are obtained from Galand et al. (2010). This recombination coefficient is modeled assuming that the magnetoshperic electrons are an additional source of ionization along with solar radiation and is in agreement within error bars of the ELS derived recombination coefficient Galand et al. (2010).

The ion charge transfer and electron attachment coefficients are calculated using the method developed by Hoppel and Frick (1986) and is shown in Fig. 2. This calculation is discussed in Michael et al. (2007, 2008, 2009) and Tripathi et al. (2008).

Initially the concentrations of positive ions and electrons are considered equal and estimated as $(q/\alpha_e)^{0.5}$. Negative ions are formed by the attachment of electrons to the neutrals. Ions and electrons are lost by the ion–ion recombination, ion–electron recombination and charge transfer to aerosols.

The differential equations are solved using the fourth-order Runge–Kutta method. This method numerically integrates ordinary differential equations using a trial step at the midpoint of an interval to cancel out lower-order error terms. This approach is used to solve the set of equations using the charge conservation as a constraint on the calculations;

$$zp + n^+ - n^- - n^e = 0 \quad (5)$$

Here n^+, n^- and n^e are the positive, negative ions and electron densities, respectively, and zp is the total charge on the aerosols, which is expressed as

$$zp = \sum_p p N_p \quad (6)$$

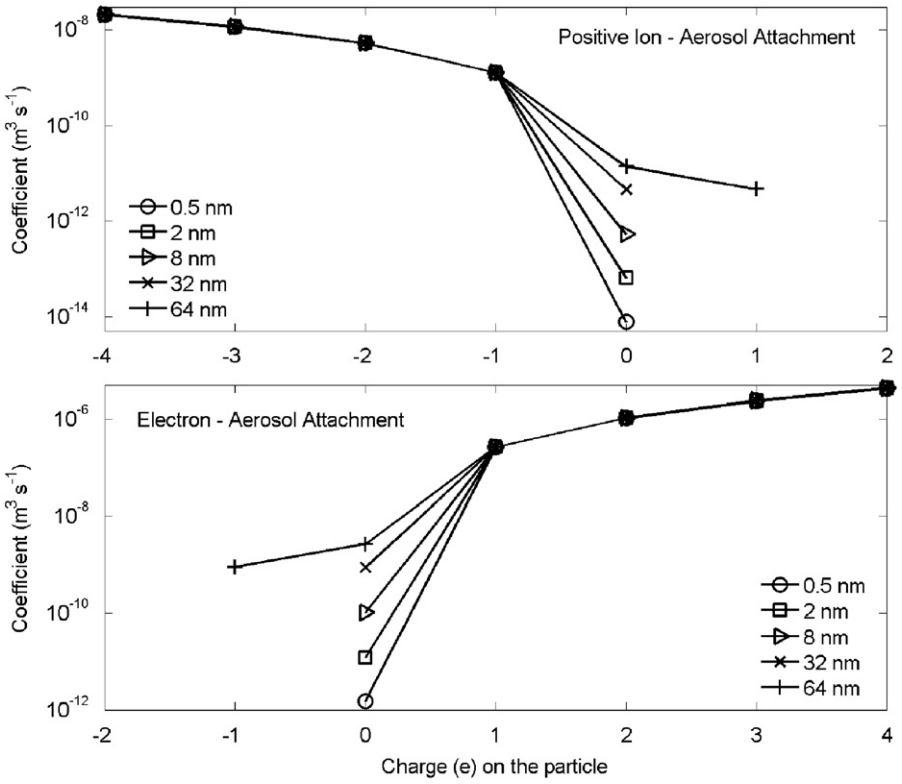

Fig. 2. Attachment coefficients of ions and electrons to aerosols of various sizes at 950 km in the atmosphere of Titan.

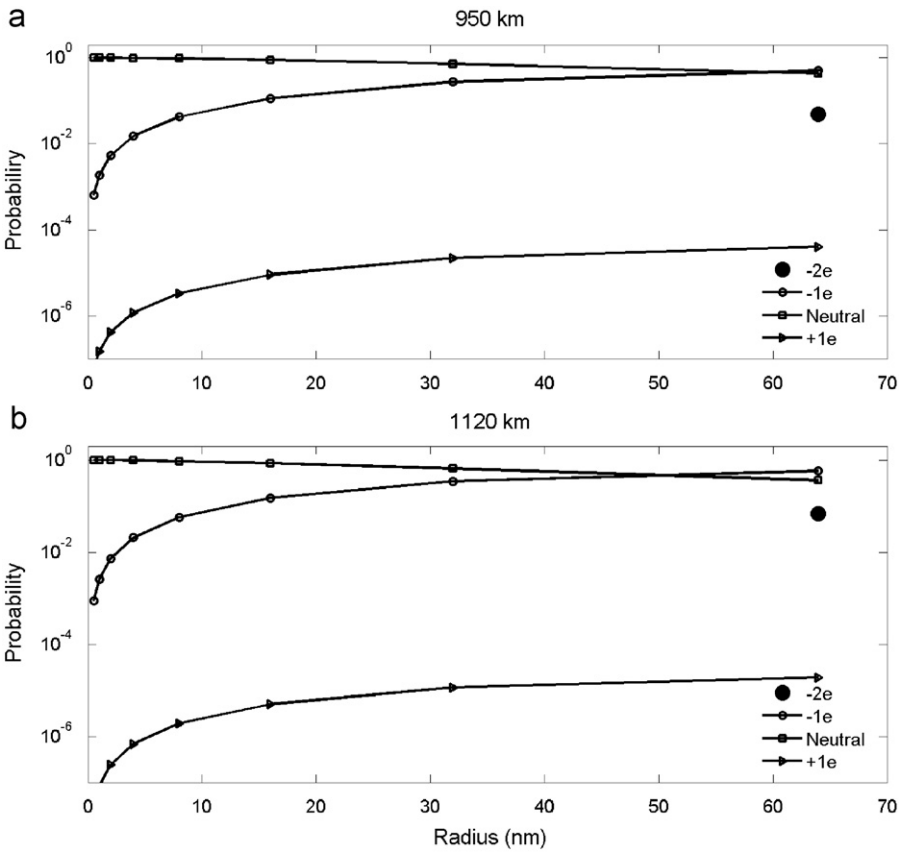

Fig. 3. (a) Probability of charging calculated at 950 km and (b) 1120 km in the atmosphere of Titan.

where N_p is the density of aerosols with charge state p. A similar numerical method was used to estimate the aerosol charging in the atmospheres of Mars (Michael et al., 2007, 2008; Michael and Tripathi, 2008), Venus (Michael et al., 2009), Titan (Borucki et al., 2006; Whitten et al., 2007) and Jupiter (Whitten et al., 2008).

3. Results and discussion

Fig. 3(a and b) shows the charge distribution in terms of probability for aerosols of different sizes at 950 km and 1120 km. Here the initial neutral aerosol concentration was taken to be 100 cm^{-3} for 950 km and 30 cm^{-3} for 1120 km with a mean radius of 8 nm for the distribution of aerosols at both the altitudes. The charge distribution probability is calculated as the ratio of the concentration of aerosols in a charge bin to the total concentration of aerosols. At 950 and 1120 km, aerosols of sizes from 0.5 to 32 nm have not more than one charge. Because the electrons are more mobile than the ions, the attachment coefficients of electrons are higher (more than two orders of magnitude) than those of ions and therefore negatively charged aerosols have a higher concentration than positively charged aerosols. The model predicts up to two charges for 64 nm aerosols with a higher concentration of negatively charged aerosols similar to that of the smaller aerosols. The probability of charging was calculated keeping the initial aerosol concentration at 50 and 2000 cm^{-3}. The results showed a maximum of 10% difference from those with an initial concentration of 100 cm^{-3}. The mass/charge has been calculated so that the concentrations can be directly compared with those measured by Coates et al. (2007) for 950 km. Though these aerosols are initially estimated to have a density of 1×10^{-3} kg/m^3 (Waite et al., 2007), later it was re-estimated that solid particles have a characteristic density of $\sim1\times10^{3}$ kgm^{-3}, whereas fractal particles have density of 1 kg/m^3 (Sittler et al., 2009; Waite et al., 2009). To calculate the mass of the aerosols, particle densities within the reported range (1, 10 and 100 kg/m^3) have been used. Though the calculations were done for an aerosol density of 1000 kg/m^3, the calculated and the observed (Coates et al., 2007) concentrations were not in agreement. As shown in Fig. 4a particle density of 1 kg/m^3 was used to calculate the mass of the aerosol and the resulting concentrations of charged aerosols are compared with T16 (Coates et al., 2007) and T29.

Different polydisperse distributions have been used with mean radii varying from 2 to 16 nm. At 950 km (Fig. 4a), the concentration of aerosols with mean radius of 2 nm is within a factor of five of the observed concentration for m/q less than 200 amu/e. Similarly, aerosol distributions with a mean radius 4 nm have a concentration, which shows agreement to some extent with the observed concentration for m/q up to 1000 amu/e. Aerosol distribution with mean radius of 8 nm have concentration, which is within an order of magnitude of the observed concentration for m/q greater than 100 amu/e. Aerosol distribution with mean radius of 16 nm have concentration, which is in agreement with the CAPS observation for m/q very close to 10,000 amu/e. Fig. 4b shows a similar plot at 1120 km in the atmosphere. The calculated concentration using the aerosol distribution with a mean radius of 2 nm shows agreement to some extent with that of the observed concentration for the whole range of observed m/q. The calculated concentration using the aerosol distribution with a

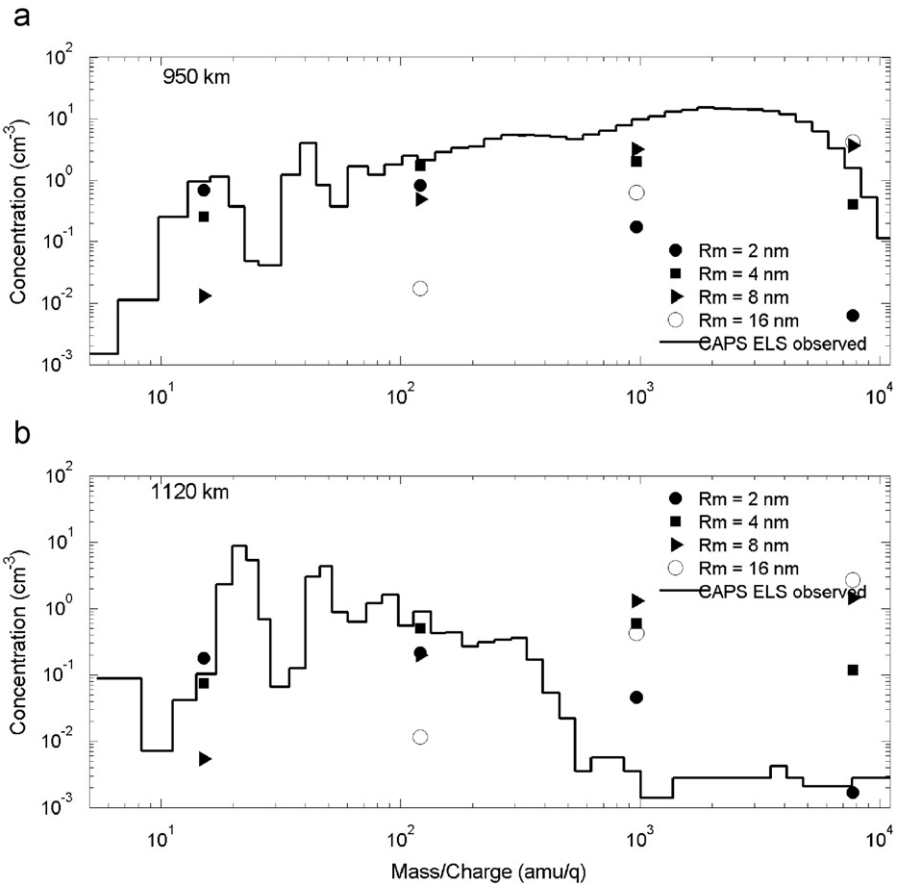

Fig. 4. Mass/charge vs. concentration calculated with a particle density of 1 kg/m^3 at (a) 950 km and (b) 1120 km. CAPS ELS spectra is from Coates et al. (2007), observed during the flyby of T16.

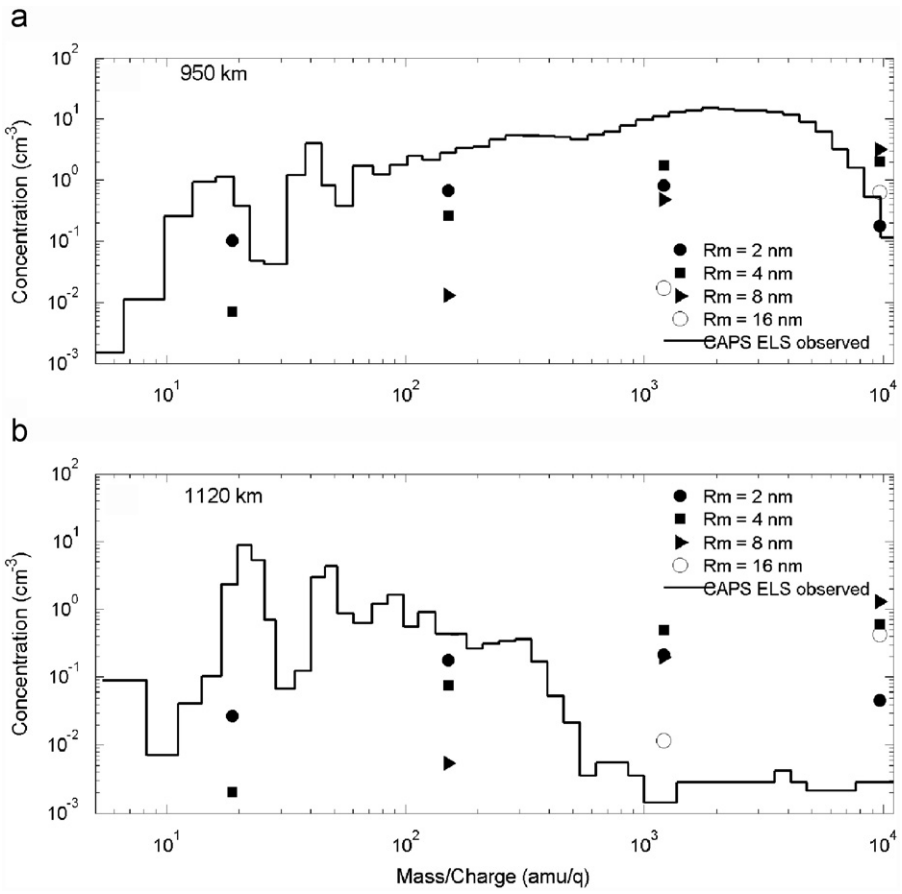

Fig. 5. Mass/charge vs. concentration calculated with a particle density of 10 kg/m^3 at (a) 950 km and (b) 1120 km. CAPS ELS spectra was observed during the flyby of T29.

mean radius of 4 and 8 nm show agreement to some extent with that of the observed concentration for m/q less than about 200 amu/e. The distribution with mean radius of 16 nm does not show any agreement with that of observation.

A particle density of 10 kg/m^3 has been used in Fig. 5(a and b). Fig. 5a and b shows the observed and calculated concentrations at 950 and 1120 km, respectively. At 950 km, the calculated concentration of aerosol distribution with mean radii 2 and 4 nm are within an order of magnitude of the observed concentration for m/q less than 200 amu/e. Calculated concentration of aerosol distribution with mean radii 8 and 16 nm, show agreement with the observed concentration only for m/q very close to 10000 amu/e. At 1120 km, none of the calculated concentrations agree with those of observed data except for distribution with mean radius of 16 nm at a m/q very close to 1000 amu/e and for distribution with mean radius 2 nm for m/q less than 200 amu/e.

Calculations made with a particle density of 100 kg/m^3 show no agreement at 950 km between the calculated and observed concentrations. At 1120 km the observed and calculated concentrations show poor agreement, except at ~1000 amu/e, where the results using the aerosol distribution with 8 nm show a difference of less than an order of magnitude with the observed concentrations.

The results presented here show that the particle density can be limited to 1–10 kg/m^3 similar to what has been reported by Sittler et al. (2009). Though aerosol distributions with mean radii 2, 4, 8 and 16 nm have been used in the present study, it is clear from Figs. 4 and 5 that the aerosol distributions with a mean radius of 16 nm are not in agreement with those of the observed data while distributions with mean radii of 2, 4 and 8 nm show agreement to some extent. In addition m/q calculations that assumed a single charge on the aerosols (Coates et al., 2007, 2009; Sittler et al., 2009) agree with our results and show that the aerosols of less than 10 nm indeed have only a single charge.

As mentioned above, the charged aerosol concentrations calculated in the present work have been compared with CAPS ELS at 950 km for T16 (Coates et al., 2007) and T29. The ELS detector is a microchannel plate (MCP) (Linder et al., 1998; Young et al., 2004), which is subject to loss in efficiency and therefore signal response for very massive ions (e.g. >1000 amu/e (Chen et al., 2003). Though there are several reasons for this falloff, the major one relevant for the ELS is detector charge saturation. The MCP operates using secondary electrons generated from the initial impact of the ion on the channel surface. The secondary electrons are accelerated through the channel and impact the channel wall, producing additional electrons leading to an electron cascade. The detector anode collects this electron cascade and generates a signal resulting in a single count). Thus the detector efficiency is directly related to the probability of production of secondary electrons. The ELS MCP is operated in saturation mode in which the electron cascade depletes the local channels of electrons and regeneration requires a period typically ~milliseconds. Since local channels are temporarily disabled they will not respond to subsequent ions or electrons collisions in the same region until it is recharged. A single heavy ion event can drive a detector into very hard saturation, making it slow to recover for the next event. When the event rates are very high (as is the case here) nearly all MCP channels can be affected in this way, which tends to cause the detector to under-count the number of events. Because the number of secondaries emitted increases with increasing ion mass, charge saturation and loss of sensitivity gets worse with an increase in aerosol mass. It should

be emphasized that while this effect is known in laboratory mass spectrometry studies of proteins and DNA, it has never before been encountered in space and so it is not surprising that this effect has not been fully taken into account in the studies reporting the detection of heavy negative ions in the atmosphere of Titan (Coates et al., 2007, 2009). The model results presented here may require some adjustment when such a correction is applied to the observations, however, it will not affect our conclusions.

4. Summary

Heavy ions (>100 amu/e), which are precursors of the aerosols in the lower atmosphere have been observed by Cassini instruments at altitudes of 950–1200 km in the atmosphere of Titan. These heavy ions of mass greater than 100 amu/e are considered aerosols and we have studied the charging of these aerosols using a one dimensional model. This study shows that aerosols of radius less than 32 nm should carry single charge while aerosols of 64 nm carry a double charge. This constraint that aerosol carries single charge is in agreement with the assumption made for the CAPS ELS observation (Coates et al., 2007, 2009). The present work estimates the particle density of 1–10 kg/m^3, similar to what has been reported by Sittler et al. (2009). The results show that aerosols must be smaller than 10 nm to get a reasonable agreement with observations by the Cassini Plasma Spectrometer.

Acknowledgment

This work was supported by grants from DST and IFCPAR Programmes. SNT was supported in part by appointment to the NASA post doctoral program at Goddard Space Flight Center.

References

Borucki, W.J., Whitten, R.C., Bakes, E.L.O., Barth, E., Tripathi, S.N., 2006. Predictions of the electrical conductivity and charging of the aerosols in Titan's atmosphere 6/20/05. Icarus 181, 527–544. doi:10.1016/j.icarus.2005.10.030.

Chen, X., Westphall, M.S., Smith, L.M., 2003. Mass spectrometric analysis of DNA mixtures: instrumental effects responsible for decreased sensitivity with increased mass. Anal. Chem. 75, 5944–5952. doi:10.1021/ac030127h.

Christophorou, L.G., 1980. Negative ions of polyatomic molecules. Environ. Health Perspect. 36, 3–32. doi:10.2307/3429329.

Coates, A.J., 2009. Interaction of Titan's ionosphere with Saturn's magnetosphere. Philos. Trans. R. Soc. A 367, 773–788. doi:10.1098/rsta.2008.0248.

Coates, A.J., et al., 2010. Negative ions at Titan and Enceladus: recent results. Faraday Discuss.. doi:10.1039/C004700G.

Coates, A.J., Crary, F.J., Lewis, G.R., Young, D.T., Waite, J.H., Sittler, E.C., 2007. Discovery of heavy negative ions in Titan's ionosphere. Geophys. Res. Lett. 34, L22103. doi:10.1029/2007GL030978.

Coates, A.J., Wellbrock, A., Lewis, G.R., Jones, G.H., Young, D.T., Crary, F.J., Waite, J.H., 2009. Heavy negative ions in Titan's ionosphere: altitude and latitude dependence. Planet. Space Sci. 57. doi:10.1016/j.pss.2009.05.009.

Crary, F.J., et al., 2009. Heavy ions, temperatures and winds in Titan's ionosphere: combined Cassini CAPS and INMS observations. Planet. Space Sci. 57. doi:10.1016/j.pss.2009.09.006.

Danielson, R.E., Caldwell, J.J., Larach, D.R., 1973. An Inversion in the Atmosphere of Titan. Icarus 20, 437. doi:10.1016/0019-1035(73)90016-X.

Galand, M., Yelle, R., Cui, J., Wahlund, J.-E., Vuitton, V., Wellbrock, A., Coates, A., 2010. Ionization sources in Titan's deep ionosphere. J. Geophys. Res. 115, A07312. doi:10.1029/2009JA015100.

Hoppel, W.A., Frick, G.M., 1986. Ion–aerosol attachment coefficients and the steady-state charge distribution on aerosols in a bipolar ion environment. Aerosol Sci. Technol. 5 (1), 1–21. doi:10.1080/02786828608959073.

Hu, H., Holzworth, R.H., 1996. Observation and parameterization of the stratospheric electrical conductivity. J. Geophys. Res. 101, 29539–29552.

Lavvas, P.P., Coustenis, A., Vardavas, I.M., 2008. Coupling photochemistry with haze formation in Titan's atmosphere. Part II: results and validation with Cassini/Huygens data. Planet. Space Sci. 56, 67–99. doi:10.1016/j.pss.2007.05.027.

Lavvas, P., Yelle, R.V., Vuitton, V., 2009. The detached haze layer in Titan's mesosphere. Icarus 201, 626–633. doi:10.1016/j.icarus.2009.01.004.

Liang, M.C., Yung, Y.L., Shemansky, D.E., 2007. Photolytically generated aerosols in the mesosphere and thermosphere of Titan. Astrophys. J. 661, L199–L202.

Linder, D.R., et al., 1998. The Cassini CAPS electron spectrometer measurement techniques for space plasmas: particles. In: Pfaff, R.F., Borovsky, J.E., Young, D.T. (Eds.), AGU Geophysical Monograph, 102; 1998, pp. 257–262.

Michael, M., Tripathi, S.N., 2008. Effect of charging of aerosols in the lower atmosphere of mars during the dust storm of 2001. Planet. Space Sci. 56, 1696–1702. doi:10.1016/J.PSS-2513.07.030.

Michael, M., Barani, M., Tripathi, S.N., 2007. Numerical predictions of aerosol charging and electrical conductivity of the lower atmosphere of Mars. Geophys. Res. Lett. 34, L04201. doi:10.1029/2006GL028434.

Michael, M., Tripathi, S.N., Mishra, S.K., 2008. Dust Charging and electrical conductivity in the day and night-time atmosphere of Mars. J. Geophys. Res. 113, E07010. doi:10.1029/2007JE003047.

Michael, M., Tripathi, S.N., Borucki, W.J., Whitten, R.C., 2009. Highly charged cloud particles in the atmosphere of Venus. J. Geophys. Res. 114, E04008. doi:10.1029/2008JE003258.

Seinfeld, J.H., Pandis, S.N., 1998. Atmospheric Chemistry and Physics: From Air Pollution to Climate Change. A Wiley-Interscience publication, USA.

Sittler, E.C., et al., 2009. Heavy ion formation in Titan's ionosphere: magnetospheric introduction of free oxygen and a source of Titan's aerosols? Planet. Space Sci. 57. doi:10.1016/j.pss.2009.07.017.

Smith, B.A., et al., 1981. Encounter with Saturn—Voyager 1 imaging science results. Science 212. doi:10.1126/science.212.4491.163.

Smith, G.R., et al., 1982. Titan's upper atmosphere composition and temperature from the EUV solar occultation results. J. Geophys. Res. 87. doi:10.1029/JA087iA03p01351.

Trafton, L.M., 1975. Near-infrared spectrophotometry of Titan. Icarus 24. doi:10.1016/0019-1035(75)90062-7.

Tripathi, S.N., Michael, M., Harrison, R.G., 2008. Profiles of ion and aerosol interactions in planetary atmospheres. Space Sci. Rev.. doi:10.1007/s11214-008-9367-7.

Tomasko, M.G., West, R.A., 2009. Aerosols in Titan's atmosphere. In: Brown, R.H., Lebreton, J.P., Waite, J.H. (Eds.), Titan from Cassini-Huygens. Springer, pp. 297–321.

Veverka, J., 1973. Titan: polarimetric evidence for an optically thick atmosphere? Icarus 18, 657. doi:10.1016/0019-1035(73)90069-9.

Vuitton, V., Lavvas, P., Yelle, R.V., Galand, M., Wellbrock, A., Lewis, G.R., Coates, A.J., Wahlund, J.-E., 2009. Negative ion chemistry in Titan's upper atmosphere. Planet. Space Sci. doi:10.1016/j.pss.2009.04.004.

Wahlund, J.-E., et al., 2005. Cassini measurements of cold plasma in the ionosphere of Titan. Science 308, 986–989. doi:10.1126/science.1109807.

Wahlund, J.E., et al., 2009. On the amount of heavy molecular ions in Titan's ionosphere. Planet. Space Sci. 57. doi:10.1016/j.pss.2009.07.014.

Waite, J.H., et al., 2005. Ion neutral mass spectrometer results from the first flyby of Titan. Science 308, 982–986. doi:10.1126/science.1110652.

Waite, J.H., et al., 2007. The process of tholin formation in Titan's upper atmosphere. Science 316, 870–875. doi:10.1126/science.1139727.

Waite, J.H., et al., 2009. High altitude production of Titan's aerosols. In: Brown, R.H., Lebreton, J.P., Waite, J.H. (Eds.), Titan from Cassini-Huygens. Springer, pp. 201–214.

Wilson, E.H., Atreya, S., 2004. Current state of modeling the photochemistry of Titan's mutually dependent atmosphere and ionosphere. J. Geophys. Res. 109, E06002. doi:10.1029/2003JE002181.

Whitten, R.C., Borucki, W.J., Tripathi, S.N., 2007. Predictions of the electrical conductivity and charging of the aerosols in Titan's nighttime atmosphere. J. Geophys. Res. 112, E04001. doi:10.1029/2006JE002788.

Whitten, R.C., Borucki, W.J., Tripathi, S.N., 2008. Predictions of the electrical conductivity and charging of the cloud particles in Jupiter's atmosphere. J. Geophys. Res. 113, E04001. doi:10.1029/2007JE002975.

Young, D.T., et al., 2004. Cassini plasma spectrometer investigation. Space Sci. Rev. 114, 1–112. doi:10.1007/s11214-004-1406-4.

Zellner, B., 1973. The polarization of Titan. Icarus 18, 661–664. doi:10.1016/0019-1035(73)90070-5.